

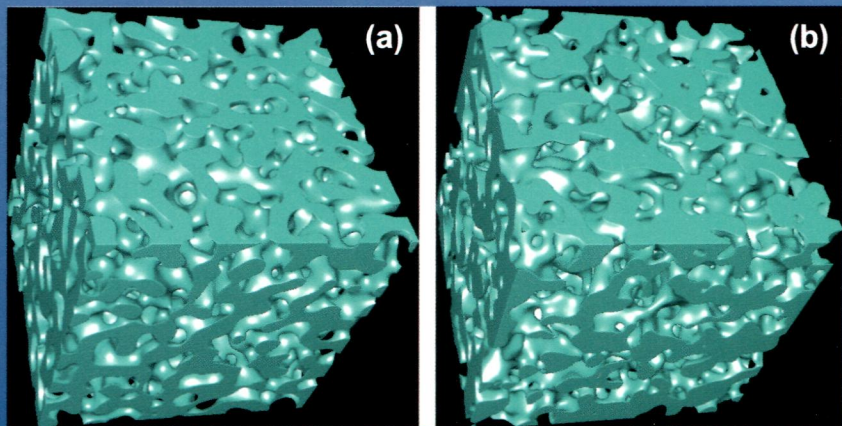
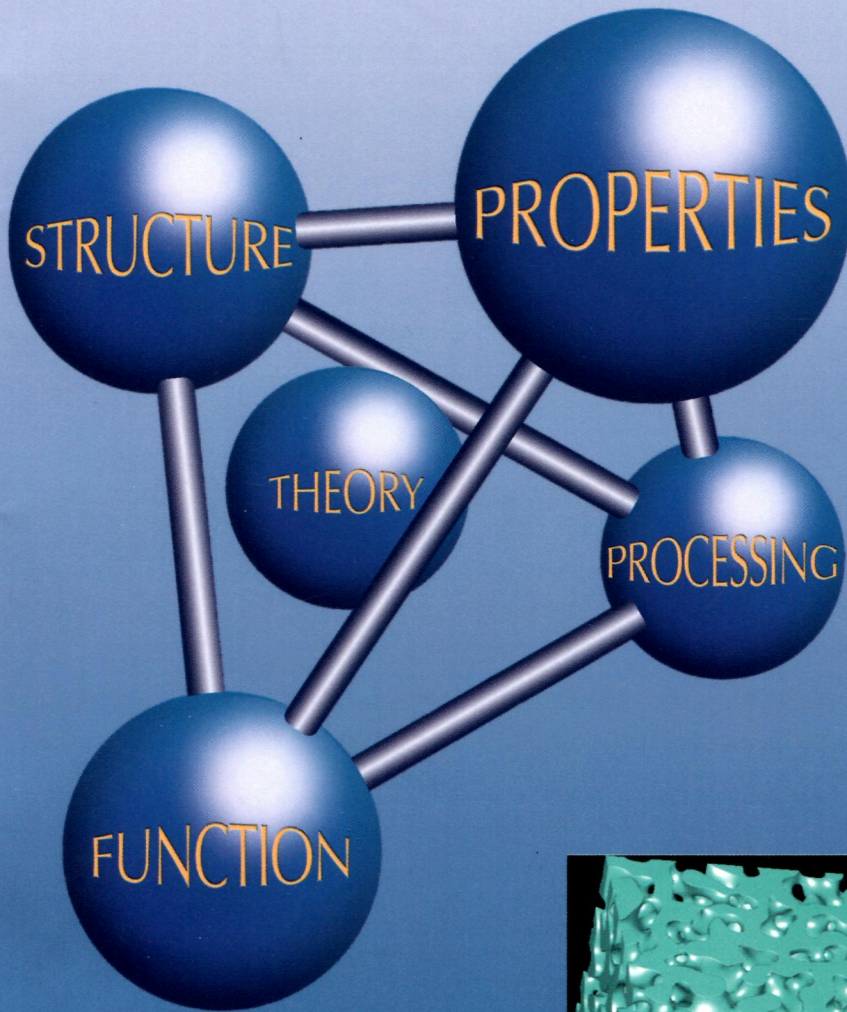
ПИ  
A 19/ma



Volume 61, Issue 1, January 2013

ISSN 1359-6454

# Acta MATERIALIA



# Acta MATERIALIA

VOLUME 61

PUBLISHED 31 OCTOBER 2012

ISSUE 1

D. W. Ji and S.-J. Kim

D. Liu, O. Lord, O. Stevens and P. E. J. Flewitt

V. Consonni, G. Rey, H. Roussel, B. Doisneau,  
E. Blanquet and D. Bellet

J. Svoboda, F. D. Fischer and W. Schillinger

O. Alshehri, M. Yavuz and T. Tsui

C. Panwisawas, H. Mathur, J.-C. Gebelin, D. Putman,  
C. M. F. Rae and R. C. Reed

T. Ezaz, J. Wang, H. Sehitoglu and H. J. Maier

H. Xu, I. Qin, H. Clauberg, B. Chylak and V. L. Acoff

S. Yang, L. Xiong, Q. Deng and Y. Chen

M. Maleki, J. Cugnoni and J. Botsis

E. F. Prados, V. L. Sordi and M. Ferrante

A. Laik, P. Mishra, K. Bhanumurthy, G. B. Kale and  
B. P. KashyapM. Tane, T. Nakano, S. Kuramoto, M. Niinomi,  
N. Takesue and H. Nakajima

- 1 Temperature-dependent ferroelastic switching of ferroelectric ceramics and evolution of linear material properties
- 12 The role of beam dispersion in Raman and photo-stimulated luminescence piezo-spectroscopy of yttria-stabilized zirconia in multi-layered coatings
- 22 Preferential orientation of fluorine-doped SnO<sub>2</sub> thin films: The effects of growth temperature
- 32 Formation of multiple stoichiometric phases in binary systems by combined bulk and grain boundary diffusion: Experiments and model
- 40 Manifestation of external size reduction effects on the yield point of nanocrystalline rhodium using nanopillars approach
- 51 Prediction of recrystallization in investment cast single-crystal superalloys
- 67 Plastic deformation of NiTi shape memory alloys
- 79 Behavior of palladium and its impact on intermetallic growth in palladium-coated Cu wire bonding
- 89 Concurrent atomistic and continuum simulation of strontium titanate
- 103 Microstructure-based modeling of the ageing effect on the deformation behavior of the eutectic micro-constituent in SnAgCu lead-free solder
- 115 The effect of Al<sub>2</sub>Cu precipitates on the microstructural evolution, tensile strength, ductility and work-hardening behaviour of a Al-4 wt.% Cu alloy processed by equal-channel angular pressing
- 126 Microstructural evolution during reactive brazing of alumina to Inconel 600 using Ag-based alloy
- 139  $\omega$  Transformation in cold-worked Ti-Nb-Ta-Zr-O alloys with low body-centered cubic phase stability and its correlation with their elastic properties

*[continued on inside back cover]*Available online at [www.sciencedirect.com](http://www.sciencedirect.com)**SciVerse ScienceDirect**

*Acta mater.* is Indexed/Abstracted in: Appl. Mech. Rev.; Res. Alert; Chem. Abstr. Serv.; Curr. Cont./Phys. Chem. Earth Sci.; Curr. Cont./Engng Tech. Appl. Sci.; Ed. Metals Abstr.; Engng Ind.; IBZ & IBR; INSPEC Data.; Metals Abstr.; PASCAL-CNRS Data.; Curr. Cont. Sci. Cit. Ind.; Curr. Cont. SCISEARCH Data.; SSSA/CISA/ECA/ISMEC; MSCI; Also covered in the abstract and citation database SciVerse Scopus®. Full text available on SciVerse ScienceDirect®.



1359-6454(201301)61:1;1-6

ISSN 1359-6454

## [CONTENTS—continued from outside back cover]

- P. Gargarella, S. Pauly, K. K. Song, J. Hu,  
N. S. Barekar, M. Samadi Khoshkhoo, A. Teresiak,  
H. Wendrock, U. Kühn, C. Ruffing,  
E. Kerscher and J. Eckert
- N. Park, A. Shibata, D. Terada and N. Tsuji
- E. Calvié, L. Joly-Pottuz, C. Esnouf, T. Douillard,  
L. Gremillard, A. Malchère, J. Chevalier and  
K. Masenelli-Varlot
- M. J. Starink, X. Cheng and S. Yang
- P. C. Wo, X. L. Zhao, P. R. Munroe, Z. F. Zhou,  
K. Y. Li, D. Habibi and Z. H. Xie
- F. Mompiou, M. Legros, A. Boé, M. Coulombier,  
J.-P. Raskin and T. Pardoën
- Z. You, X. Li, L. Gui, Q. Lu, T. Zhu, H. Gao and  
L. Lu
- K. Sitarama Raju, V. Subramanya Sarma,  
A. Kauffmann, Z. Hegedüs, J. Gubicza,  
M. Peterlechner, J. Freudenberger and G. Wilde
- F. Wakai
- F. Cernuschi, I. O. Golosnoy, P. Bison, A. Moscatelli,  
R. Vassen, H.-P. Bossmann and S. Capelli
- P. Ranzieri, S. Fabbrici, L. Nasi, L. Righi, F. Casoli,  
V. A. Chernenko, E. Villa and F. Albertini
- T. Yuan, G. Wang, Q. Feng, P. K. Liaw,  
Y. Yokoyama and A. Inoue
- A. R. P. Singh, S. Nag, S. Chattopadhyay, Y. Ren,  
J. Tiley, G. B. Viswanathan, H. L. Fraser and  
R. Banerjee
- Y. Kamimura, K. Edagawa and S. Takeuchi
- J. Trapp and B. Kieback
- D. D. Qu, K.-D. Liss, Y. J. Sun, M. Reid, J. D. Almer,  
K. Yan, Y. B. Wang, X. Z. Liao and J. Shen
- F. Siska, M. Ramajayam, D. Fabijanic and M. Barnett
- H. Gholizadeh, C. Draxl and P. Puschnig
- Z. Yang, M. F. Chisholm, G. Duscher, X. Ma and  
S. J. Pennycook
- F. Wang, Z. Liu, D. Qiu, J. A. Taylor,  
M. A. Easton and M.-X. Zhang
- A. Kuzmin, A. Kalinko and R. A. Evarestov
- K. Dey, S. Majumdar and S. Giri
- F.-X. Li and K.-J. Kang
- 151 Ti–Cu–Ni shape memory bulk metallic glass composites
- 163 Flow stress analysis for determining the critical condition of dynamic ferrite transformation in 6Ni–0.1C steel
- 174 Evidence for the formation of distorted nanodomains involved in the phase transformation of stabilized zirconia by coupling convergent beam electron diffraction and in situ TEM nanoindentation
- 183 Hardening of pure metals by high-pressure torsion: A physically based model employing volume-averaged defect evolutions
- 193 Extremely hard, damage-tolerant ceramic coatings with functionally graded, periodically varying architecture
- 205 Inter- and intragranular plasticity mechanisms in ultrafine-grained Al thin films: An in situ TEM study
- 217 Plastic anisotropy and associated deformation mechanisms in nanotwinned metals
- 228 High strength and ductile ultrafine-grained Cu–Ag alloy through bimodal grain size, dislocation density and solute distribution
- 239 Mechanics of viscous sintering on the micro- and macro-scale
- 248 Microstructural characterization of porous thermal barrier coatings by IR gas porosimetry and sintering forecasts
- 263 Epitaxial Ni–Mn–Ga/MgO(100) thin films ranging in thickness from 10 to 100 nm
- 273 Modeling size effects on fatigue life of a zirconium-based bulk metallic glass under bending
- 280 Mechanisms related to different generations of  $\gamma'$  precipitation during continuous cooling of a nickel base superalloy
- 294 Experimental evaluation of the Peierls stresses in a variety of crystals and their relation to the crystal structure
- 310 Solid-state reactions during high-energy milling of mixed powders
- 321 Structural origins for the high plasticity of a Zr–Cu–Ni–Al bulk metallic glass
- 331 Internal material “architecture” for a kink-resistant metal tube
- 341 The influence of interstitial carbon on the  $\gamma$ -surface in austenite
- 350 Direct observation of dislocation dissociation and Suzuki segregation in a Mg–Zn–Y alloy by aberration-corrected scanning transmission electron microscopy
- 360 Revisiting the role of peritectics in grain refinement of Al alloys
- 371 Ab initio LCAO study of the atomic, electronic and magnetic structures and the lattice dynamics of triclinic CuWO<sub>4</sub>
- 379 Structural correlation to magnetodielectricity and coercivity at room temperature in multiferroic Bi<sub>0.7</sub>Ba<sub>0.3-x</sub>Pb<sub>x</sub>FeO<sub>3</sub>
- 385 Deformation and cracking near a hole in an oxide-forming alloy foil subjected to thermal cycling